Comparative Molecular Similarity Index Analysis on 2-(indol-5-yl)thiazolederivatives as Xanthine Oxidase(XO)inhibitors

Santhosh Kumar Nagarajan and Thirumurthy Madhavan[†]

Abstract

Xanthine Oxidase is an enzyme, which oxidizes hypoxanthine to xanthine, and xanthine to uric acid. It is widely distributed throughout various organsincluding the liver, gut, lung, kidney, heart, brain and plasma. It is involved in gout pathogenesis. In this study, we have performed Comparative Molecular Field Analysis (CoMSIA) on a series of 2-(indol-5-yl) thiazole derivatives as xanthine oxidase (XO) inhibitors to identify the structural variations with their inhibitory activities. Ligand based CoMSIA models were generated based on atom-by-atom matching alignment. In atom-by-atom matching, the bioactive conformation of highly active molecule 11 was generated using systematic search. Compounds were aligned using the bioactive conformation and it is used for model generation. Different CoMSIA models were generated using different alignments and the best model yielded across-validated q^2 of 0.698 with five components and non-cross-validated correlation coefficient (r^2) of 0.992 with Fisher value as 236.431, and an estimated standard error of 0.068. The predictive ability of the best CoMSIA models was found to be r^2_{pred} 0.653. The study revealed the important structural features required for the biological activity of the inhibitors and could provide useful for the designing of novel and potent drugs for the inhibition of Xanthine oxidase.

Keywords: Xanthine Oxidase, Gout, 3D-QSAR, CoMSIA.

1. Introduction

Xanthine oxidase is an enzyme that generates reactive oxygen species. The enzyme oxidizes hypoxanthine to xanthine, and xanthine to uric acid, producing hydrogen peroxide. XO is widely distributed throughout various organs such as the liver, gut, lung, kidney, heart, brain and plasma[1]. High level of XO secretion is found in the gut and the liver[2]. It is localized to the capillary endothelial cells, in the myocardium[3]. It is capable of catalyzing the formation of urate in man[4]. There is a large variability in human XOR expression which can be up to three-fold and on average 20% higher in men than in women[5].

The active form of the enzyme is a homodimer. The molecular mass of the enzyme is 290 kDa. Each monomer of the homodimer acts independently in catalysis.

In each subunit molecule, an N-terminal 20-kDa domain containing two iron sulfur centers is present. A central 40-kDa FAD domain and a C-terminal 85-kDa molybdopterin-binding domain with the four redox centers aligned in an almost linear fashion are also present. The hydroxylation of xanthine takes place at the molybdopterin center. Thus, the electrons introduced are rapidly transferred to the other linearly aligned redox centers[6,7].

Xanthine oxidase is involved in gout pathogenesis. In gout, defective metabolism of uric acid causes arthritis, especially in the smaller bones of the feet and deposition of chalk-stones. This causes episodes of acute pain in patients. According to the Third National Health and Nutrition Examination Survey (1988–1994), gout is a prevalent disease with occurrence of >2% in men older than 30 years and in woman older than 50 years[8,9]. It occurs in individuals who have high serum uric acid levels, in response to precipitation of monosodium uratemonohydate crystals in various tissues, followed by an inflammatory response. Typical symptoms include acute recurrent gouty arthritis, a tophinodular collection of monosodium urate crystals and uric acid

Department of Genetic Engineering, School of Bioengineering, SRM University, SRM Nagar, Kattankulathur, Chennai 603203, India

[†]Corresponding author : thiru.murthyunom@gmail.com, thirumurthy.m@ktr.srmuniv.ac.in

urolithiasis[10]. XO also plays an important role in various forms of ischemic and other types of tissue and vascular injuries, inflammatory diseases, and chronic heart failure[11].

Xanthine oxidase inhibitor is any substance that inhibits the activity of xanthine oxidase. There are two kind of Xanthine oxidase inhibitors: purine analogues and others. Purine analogues include allopurinol, oxypurinol, and tisopurine. Others include febuxostat, topiroxostat, and inositols (phytic acid and myo-inositol). These commercially available drugs have certain disadvantages. For Example, Allopurinol has two important disadvantages. First, its dosing is complex[12]. Second, some patients are hypersensitive to the drug,[13] therefore its use requires careful monitoring. Allopurinol has rare but potentially fatal adverse effects involving the skin. The most serious adverse effect is a hypersensitivity syndrome consisting of fever, skin rash,

eosinophilia, hepatitis, worsened renal function, and, in some cases, allopurinol hypersensitivity syndrome[13]. The adverse effects of febuxostat include nausea, diarrhea, arthralgia, headache, increased hepatic serum enzyme levels and rash[14]. Hence, the discovery of structurally diverse XO inhibitors and analyzing the important structural properties required for their biological activity becomes important.

2. Materials and Methods

2.1. Data Set

A series of 21 compounds with their biological activities were taken from the literature[15]. The compounds were divided into training set and test set molecules. The test set molecules were selected manually in order to cover low, middle, and high biological activity from the dataset. For CoMSIA

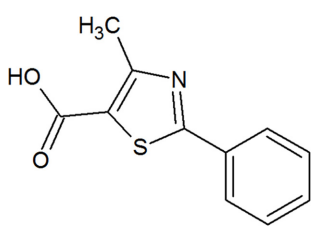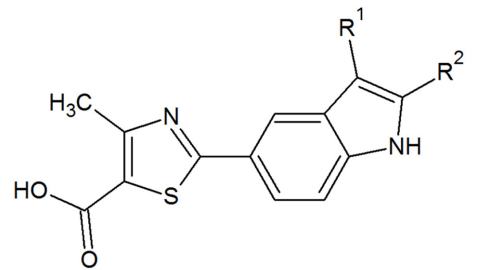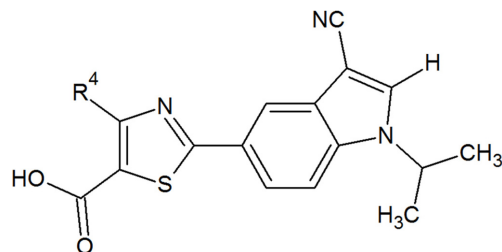**Table 1.** Structures and biological activities (pIC$_{50}$) of Xanthine Oxidase inhibitors
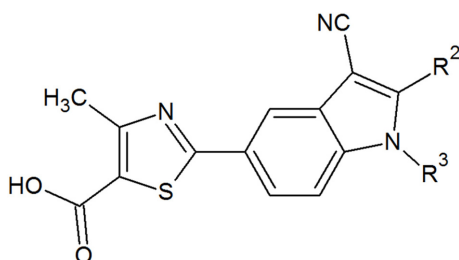
The Xanthine Oxidase inhibitor scaffold

a) Compound 1-7

Compound	R^1	R^2	pIC50 values
1	H	H	6.9586
2	Cl	H	7.9706
3	Cl	H	8.5529
4	Cl	CH$_3$	8.0458
5	NO$_2$	H	7.9101
6	NO$_2$	H	8.2518
7	CN	H	8.2218

Table 1. Continued

b) Compound 8-11

Compound	R^4	pIC50 values
8	H	8.4089
9	CF_3	8.0655
10	OCH_3	7.0457
11	CH_3	8.2441

c) Compound 12-21

Compound	R^2	R^3	pIC50 values
12	H	2-methylpropane	7.7959
13	CH_3	1-fluoro-2-methylpropane	8.3767
14	H	2-methylpropan-1-ol	7.9208
15	H	1-methoxy-2-methylpropane	8.2596
16	H	1-(methylsulfonyl)propane	8.3565
17	H	N-propylacetamide	6.0482
18	H	N-propylmethanesulfonamide	7.0458
19	H	ethylbenzene	8.4559
20	H	1-ethyl-2,4-difluorobenzene	8.320

d) Febuxostat

Compound	Structure	pIC50 values
21		8.2596

analysis, the given inhibitory concentration values (IC$_{50}$) were changed to minus logarithmic scale value (pIC$_{50}$), as a dependent variable for 3D-QSAR analysis.

$$pIC_{50} = -\log (IC_{50}).$$

The structures and biological activities of all compounds including both training set and test set molecules is shown in Table 1.

2.2. Partial Atomic Charge Calculation and Bioactive Conformation Determination

For each compound, the partial atomic charges were assigned by utilizing Gasteiger-Hückel method available in SYBYLX 2.1 package (Tripos Inc., St. Louis, MO, USA). The bioactive conformation of the highly active compound 11 was determined using systematic search method. The obtained conformation from these methods was used as the template to perform alignment for CoMSIA calculations. During systematic search all rotatable bonds were searched with incremental dihedral angle from 120° and the lowest energy conformer was assumed as bioactive conformer and was chosen for subsequent QSAR modeling. Bioactive conformations for other compounds were determined by systematic conformer search for the additional moieties, by keeping core part constrained. It was seen that, the common scaffold of every inhibitor occupies the same area in 3D space. The matching atoms were selected by maximum common substructure (MCS) as shown in Fig. 1(a) and the alignment of all the molecules are represented in Fig. 1(b).

2.3. CoMSIA Model Calculation

CoMSIA was performed with the generally used steric, electrostatic, hydrophobic, H bond donor and acceptor fields in SYBYL-X 2.0. The aim of CoMSIA analysis is to derive a correlation between the biological activity of a set of molecules and their 3D shape, electrostatic and hydrogen bonding characteristics. This correlation is derived from a series of superimposed conformations aligned using the atom-by-atom matching. Each conformation is taken in turn, and the molecular fields around it are calculated. The electrostatic and steric (van der Waals interactions) fields are measured at the lattice points of a regular Cartesian 3D grid. The lattice spacing is typically 2 Å. The lattice was defined
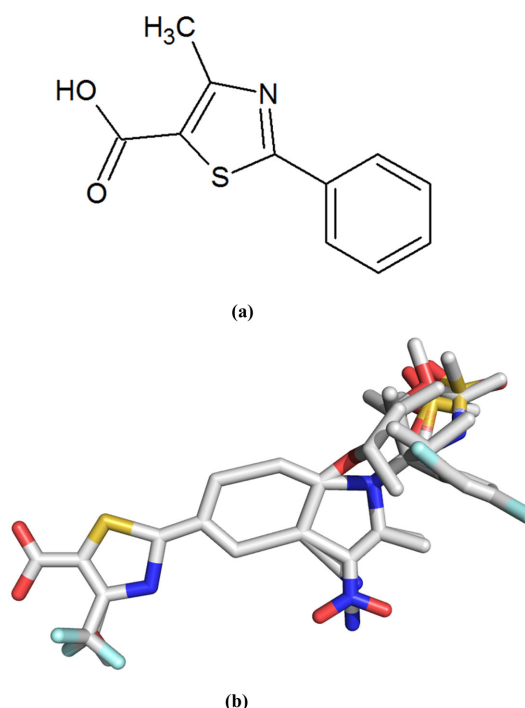

(a)

(b)

Fig. 1. (a) Maximum common substructure present in all molecules. (b) Alignment of molecules based on systematic search conformation of highly active compound 11.

automatically and is extended 4 units past Van der Waals volume of all molecules in x, y, and z directions. Using Tripos force field, the Van der Waals potential and columbic terms, which represent steric and electrostatic fields, respectively, were calculated. A distance-dependent dielectric constant was used. The CoMSIA method was performed with standard ±30 kcal/mol cut-offs. A series of models were constructed with an increasing number of partial least squares (PLS) analysis factors. The numbers of components in the PLS models were optimized by using the cross-validated correlation coefficient (q^2), non-cross-validated correlation coefficient (r^2), standard error estimate (SEE) and Fisher's values (F), etc., which were obtained from the leave-one-out (LOO) cross-validation procedures[16,17]. After the optimal number of components was determined, a non-cross-validated analysis was carried out without column filtering.

2.4. Partial Least Squares (PLS) Analysis

The CoMSIA equation was established by partial least-squares (PLS) analysis between biological activity

and molecular parameters. By using the PLS method[18,19] the CoMSIA descriptors were linearly correlated with the biological activity values. The CoMSIA cutoff values were set to 30 kcal/mol for both the steric and electrostatic fields. Leave-one-out method (LOO Method) was used to perform the cross-validation analysis. The cross-validated correlation coefficient (q^2) was calculated using the following equation:

$$q^2 = 1 - \frac{\sum_{\gamma}(\gamma_{pred} - \gamma_{actual})^2}{\sum_{\gamma}(\gamma_{actual} - \gamma_{mean})^2}$$

where γ_{pred}, γ_{actual}, and γ_{mean} are the predicted, actual, and mean values of the target property (pIC_{50}), respectively.

2.5. Predictive Correlation Coefficient (r^2_{pred})

The predictive power of CoMSIA models were determined from the set of six test molecules which was excluded during model development. In the structural preparation of test set molecules, sketching and optimization was same as the training set molecules. The activity of the test set was predicted by using model

derived from training set. The predictive correlation coefficient (r^2_{pred}), based on the test set molecules, is defined as:

$$r^2_{pred} = \frac{(SD - PRESS)}{SD}$$

where, PRESS is the sum of the squared deviation between the predicted and actual activity of the test set molecules, and SD is defined as the sum of the square deviation between the biological activity of the test set compounds and the mean activity of the training set molecules.

2.6. CoMSIA Contour Maps

CoMSIA analysis generates color-coded contour maps that represent regions in three dimensional space where changes in the steric and electrostatic fields of a compound correlate strongly with changes in its biological activity. Contour maps were generated as a scalar product of coefficients and standard deviation(StDev * Coeff) associated with each column. Favored levels were fixed at 80% and disfavoured levels were fixed at 20%. The contours for steric fields are shown in green

Table 2. Statistical results of CoMSIA models obtained from systematic search conformation based alignment

PLS statistics	Ligand-based CoMSIA model (systematic search)				
	Model1	Model2	Model3	Model4	Model5
q^2	0.635	0.512	0.561	0.488	0.462
N	4	6	6	6	3
r^2	0.958	0.987	0.997	0.985	0.978
SEE	0.160	0.101	0.050	0.104	0.108
F-value	57.598	98.865	422.816	90.064	75.328
r^2_{pred}	0.659	0.587	0.597	0.512	0.498
Field contribution					
Steric	0.076	0.071	0.064	0.071	0.067
Electro static	0.207	0.223	0.241	0.220	0.141
Acceptor	0.103	0.116	0.119	0.117	0.137
Hydrophobic	0.107	0.111	0.116	0.117	0.157
Donor	0.507	0.479	0.461	0.475	0.498

q^2= cross-validated correlation coefficient; N= number of statistical components; r^2= non-cross validated correlation coefficient; SEE=standard estimated error; F=Fisher value; $r^2_{predictive}$= predictive correlation coefficient for test set. The model chosen for analysis is highlighted in bold fonts.
Test set compounds
Model1- compound no 1,3,9,13,15,16
Model2 - compound no 1,3,9,13,16,21
Model3 - compound no 1,3,9,12,13,16
Model 4 - compound no 1,3,9,13,16,19
Model5 - compound no 1,5,9,13,15,16

(more bulk favored) and yellow (less bulk favored). The electrostatic field contours are displayed in red (electronegative substitutions favored) and blue (electropositive substitutions favored) colors. The hydrophobic field contours are displayed in yellow (hydrophobic substitutions are favourable) and white (hydrophobic substitutions are unfavourable) colors. The H-bond donor field contours are displayed in cyan (hydrogen bond donor substitutions enhance activity) and purple (hydrogen bond donor substitutions reduce activity) colors. The H-bond acceptor field contours are displayed in magenta (hydrogen bond acceptor group enhance activity) and red (hydrogen bond acceptor group reduce activity) colors.

3. Results and Discussion

In the present work, ligand-based CoMSIA models was generated on a series of 2-(indol-5-yl) thiazole derivatives as xanthine oxidase inhibitors. Different combinations of 15 training and 6 test compounds were used for model generation. Alignment was based on atom-by-atom matching method. Many CoMSIA models were obtained, of those only 5 models from systematic search conformation were selected based on higher q^2 and r^2_{pred} values.

3.1. CoMSIA Model Analysis
Ligand-based CoMSIA models was generated using different combinations of training set and test compounds.Based on higher q^2 and r^2_{pred} values only 5 models from systematic search were selected. The

Table 3. Predicted activities and experimental pIC_{50} values obtained from CoMSIA models

Compound	Actual pIC_{50}	Predicted	Residual
1*	6.959	7.34	-0.381
2	7.971	7.809	0.162
3*	8.553	8.717	-0.164
4	8.046	8.212	-0.166
5	7.910	7.757	0.153
6	8.252	8.344	-0.092
7	8.222	8.291	-0.069
8	8.409	8.349	0.06
9*	8.065	7.755	0.31
10	7.046	7.231	-0.185
11	8.244	8.108	0.136
12	7.796	8.079	-0.283
13*	8.377	8.332	0.045
14	7.921	7.869	0.052
15*	8.260	8.074	0.186
16*	8.356	8.475	-0.119
17	6.048	6.077	-0.029
18	7.0456	6.949	0.0966
19	8.456	8.339	0.117
20	8.320	8.287	0.033
21	8.260	8.244	0.016

*Test set compounds

statistical values of the 5 models from different alignments are tabulated in Table 2 for systematic search. The best statistics were found in Model 1 having a cross-validated q^2 of 0.635 with four components and non-cross-validated correlation coefficient (r^2) of 0.958
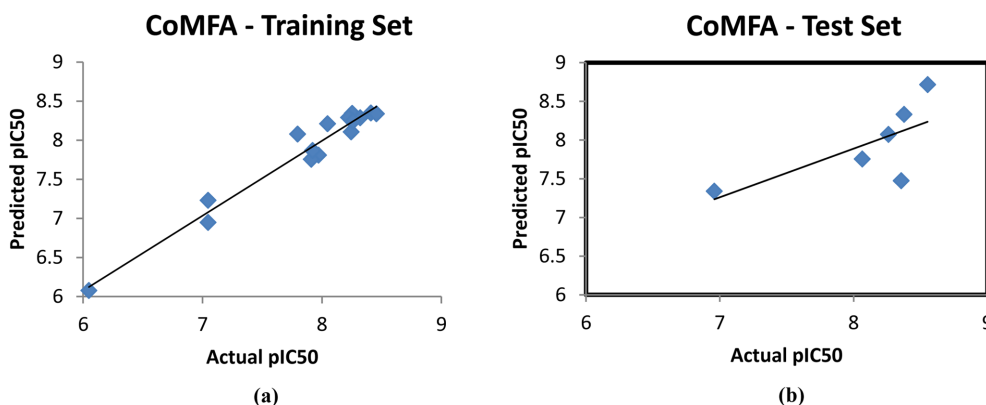

Fig. 2. (a and b) Plot of actual versus predicted pIC50 values for the training set and test set for the CoMSIA values performed after atom-by atom matching alignment by systematic search.

with Fisher value as 57.598, and an estimated standard error of 0.160. The predictive ability of the best CoMSIA models was found to be r^2_{pred} 0.659.Predicted and experimental pIC_{50} and their residual values in Table 3 and their corresponding scatter plot is depicted in Fig. 2.

3.2. Mapping of CoMSIA Contour Maps

The CoMSIA contour map for the generated models was analysed to explore the important structural features. The steric, electrostatic, hydrophobic, H bond donor and acceptor contour maps obtained for systematic search alignment based CoMSIA model are displayed in Fig. 3, 4, 5, 6 and 7 respectively. Steric and electrostatic contour maps are in correspondence with

the CoMFA studies on the same dataset previously reported by us[20]. Steric interactions are represented by green and yellow contours. The green steric contour near the R_3 position indicates that bulkier substitutions are preferred at this position. Compounds 6, 20 and 21 with bulkier substitutions at these positions are more active than compounds which have smaller substitutions at the R_3 position. Electrostatic interactions are represented by red and blue contours. The blue contours represent that the electropositive substitutions are favored in that region. The electrostatic contour plot shows that there is a big blue coloredregion near the R_3 position. Electro positive group linked to this position will enhance the biological activity. Compounds 16, 17 and 18 having electropositive substitutions at that position,
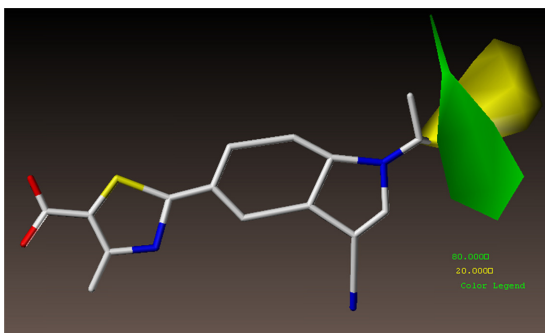

Fig. 3. CoMSIA steric contour map with highly active compound 11 for systematic search based alignment. Here green contour indicates region where bulky group increases activity and yellow contours indicates bulky group decreases activity.
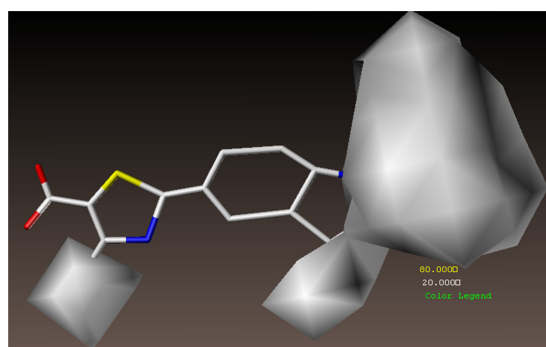

Fig. 5. CoMSIA hydrophobic contour map with highly active compound 11 for systematic search based alignment. In hydrophobic field contour, yellow contour map indicates the region where the hydrophobic substitutions are favourable for activity and white contour indicates the disfavoured region for inhibitory activity.
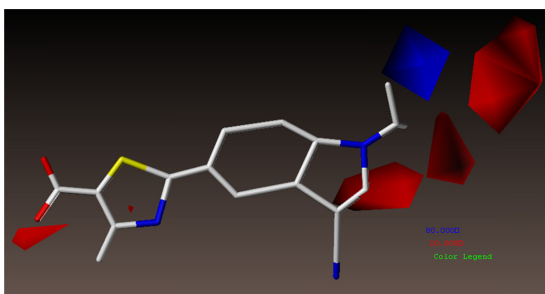

Fig. 4. CoMSIA electrostatic contour map with highly active compound 11 for systematic search based alignment. Here blue contour indicates regions where electropositive groups increases activity and red contours indicates regions where electronegative groups increases activity.
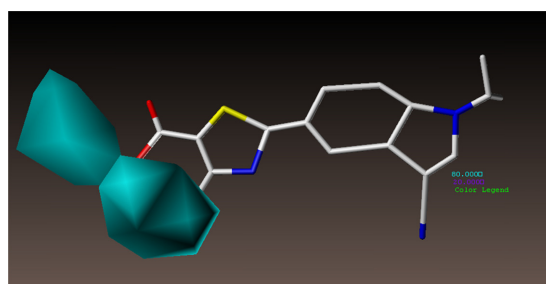

Fig. 6. CoMSIA H-bond donor contour map with highly active compound 11 for systematic search based alignment. Cyan indicates regions where hydrogen bond donor substitutions enhance activity; purple indicates hydrogen bond donor substitutions reduce activity.
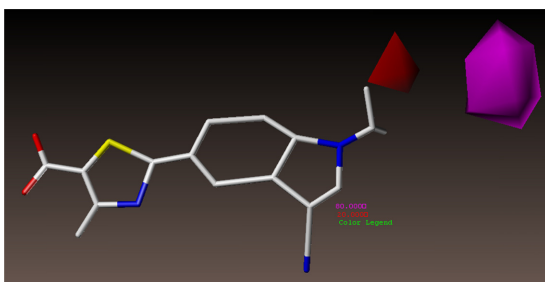
Fig. 7. CoMSIA H-bond acceptor contour map with highly active compound 11 for systematic search based alignment. Magenta contour map indicates where hydrogen bond acceptor group increases the activity and red contour map indicates the hydrogen bond acceptor group decreases the activity.

such as 1-(methylsulfonyl)propane, N-propylacetamide and N-propylmethanesulfonamide respectively, is in direct contact with the big blue contour map. The red contours represent that the electronegative substitutions are favored in that region. For example, the substitutions at theR3 position of compounds 1 and 20 are in direct contact with the red contour map, which reduce the biological activity. In hydrophobic contour map, yellow contour indicates the regions were hydrophobic substitutions are favorable and white contour represent that the hydrophobic substitutions are unfavorable for inhibitory activity at that position. A large white region can be seen around the phenyl ring which denotes the importance of the absence of hydrophobic substitutions around that position. None of the compounds with higher activity have hydrophobic substitutions at the region. In H bond donor contour maps, cyan color contours represent the regions where H bond donor substitutions enhance the biological activity and purple regions indicate the H bond donor group reduces the activity. Two big cyan colored regions are present around the R^4 position. Compounds like 8, 9 and 11 with H bond donor groups at the position have higher activity. In H bond acceptor contour maps, magenta contours indicate the regions where H bond acceptor substitutions increase the biological activity and red contours represent the regions where H bond acceptor group reduces the activity. A red contour can be seen near the R^3 substitution position of the phenyl ring. Hence, compounds with H bond acceptor groups at that position, like 14, 17 and 18 have lower activity.

4. Conclusion

In this study, we have developed CoMSIA models of 2-(indol-5-yl) thiazole derivatives as xanthine oxidase inhibitors. CoMSIA models with good cross-validated q^2 values and predictive ability were obtained. The statistical results showed the important structural alignments required for the inhibitory activity of the 2-(indol-5-yl) thiazole derivatives. The results correlate the structural features with the inhibitory activities against xanthine oxidase and provide valuable information about characteristics of inhibitors. The present CoMSIA study revealed that the R_3 position of the structure is important in influencing the biological activity of the inhibitors. Electro positive groups and bulkier substitutions linked to this position enhances the biological activity. The results obtained from this study could provide the required structural and chemical features in designing and developing new potent novel inhibitors for xanthine oxidase.

Conflict of interest
The authors declare that they have no conflict of interest.

References

[1] P. Pacher, A. Nivorozhkin, and C. Szabó, "Therapeutic effects of xanthine oxidase inhibitors: renaissance half a century after the discovery of allopurinol", Pharmacol. Rev., Vol. 58, pp. 87-114, 2006.

[2] D. A. Parks and D. N. Granger, "Xanthine oxidase: biochemistry, distribution and physiology", Acta Physiologica Scandinavica. Supplementum, Vol. 548, pp. 87-99, 1986.

[3] M. Cicoira, L. Zanolla, A. Rossi, G. Golia, L. Franceschini, G. Brighetti, P. Zeni, and P. Zardini, "Elevated serum uric acid levels are associated with diastolic dysfunction in patients with dilated cardiomyopathy", Am. Heart J., Vol. 143, pp. 1107-1111, 2002.

[4] K. D. Pfeffer, T. P. Huecksteadt, and J. R. Hoidal, "Xanthine dehydrogenase and xanthine oxidase activity and gene expression in renal epithelial cells. Cytokine and steroid regulation", J. Immunol., Vol. 153, pp. 1789-1797, 1994.

[5] R. Guerciolini, C. Szumlanski, and R. M. Weinshilboum, "Human liver xanthine oxidase: nature and

extent of individual variation", Clin. Pharmacol. Ther., Vol. 50, pp. 663-672, 1991.

[6] R Harrison, "Structure and function of xanthine oxidoreductase: where are we now?", Free Radical Biol. Med., Vol. 33, pp. 774-797, 2002.

[7] R Harrison, "Physiological roles of xanthine oxidoreductase", Drug Metab. Rev., Vol. 36, pp. 363-375, 2004.

[8] H. M. Kramer and G. Curhan, "The association between gout and nephrolithiasis: the national health and nutrition examination survey III, 1988-1994", Am. J. Kidney Dis., Vol. 40, pp. 37-42, 2002.

[9] H. K. Choi and G. Curhan, "Gout: epidemiology and lifestyle choices", Curr. Opin. Rheumatol., Vol. 17, pp. 341-345, 2005.

[10] R. L. Wortmann, "Recent advances in the management of gout and hyperuricemia", Curr. Opin. Rheumatol., Vol. 17, pp. 319-324, 2005.

[11] J. George and A. D. Struthers, "The role of urate and xanthine oxidase inhibitors in cardiovascular disease", Cardiovasc. Ther., Vol. 26, pp. 59-64, 2008.

[12] N. Dalbeth and L. Stamp, "Allopurinol Dosing in Renal Impairment: Walking the Tightrope Between Adequate Urate Lowering and Adverse Events", Semin. Dialysis, Vol. 20, pp. 391-395, 2007.

[13] T.-F. Tsai and T.-Y. Yeh, "Allopurinol in dermatology", Am. J. Clin. Dermatol., Vol. 11, pp. 225-232, 2010.

[14] B. L. Love, R. Barrons, A. Veverka, and K. M. Snider, "Urate-lowering therapy for gout: focus on febuxostat", Pharmacotherapy, Vol. 30, pp. 594-608, 2010.

[15] J. U. Song, S. P. Choi, T. H. Kim, C.-K. Jung, J.-Y. Lee, S.-H. Jung, and G. T. Kim, "Design and synthesis of novel 2-(indol-5-yl)thiazole derivatives as xanthine oxidase inhibitors", Bioorg. Med. Chem. Lett., Vol. 25, pp. 1254-1258, 2015.

[16] K. Abe, H. Shimokawa, K. Morikawa, T. Uwatoku, K. Oi, Y. Matsumoto, T. Hattori, Y. Nakashima, K. Kaibuchi, K. Sueishi, and A. Takeshit, "Long-term treatment with a Rho-kinase inhibitor improves monocrotaline-induced fatal pulmonary hypertension in rats", Circ. Res., 94: 385-393, 2004.

[17] T. Ishizaki, M. Uehata, I. Tamechika, J. Keel, K. Nonomura, M. Maekawa, and S. Narumiya, "Pharmacological Properties of Y-27632, a Specific Inhibitor of Rho-Associated Kinases", Mol. Pharmacol., Vol. 57, pp. 976-983, 2000.

[18] P. Geladi and B. Kowalski, "Partial least-squares regression: a tutorial", Anal. Chim. Acta, Vol. 185, pp. 1-17, 1986.

[19] S. Wold, "Cross-validatory estimation of the number of components in factor and principal components models", Technometrics, Vol. 20, pp. 397-405, 1978.

[20] N. Santhosh Kumar and M. Thirumurthy, "3D-QSAR Studies on 2-(indol-5-yl)thiazole Derivatives as Xanthine Oxidase (XO) Inhibitors", J. Chosun Natural Sci., Vol. 8, pp. 258-266, 2015.